Journal of Nuclear Medicine, published on March 10, 2022 as doi:10.2967/jnumed.121.262928

Heterogeneity of SSTR2 expression assessed by ^{68}Ga-DOTATOC-PET/CT using coefficient of variation in patients with neuroendocrine tumors.

AUTHORS: Rosa Fonti [1,2], Mariarosaria Panico[1,2], Sara Pellegrino[2], Alessandro Pulcrano[2], Luisa Alessia Vastarella[2], Armin Hakkak[2], Mario Giuliano[3,4], Giovannella Palmieri[4], Sabino De Placido[3,4], Silvana Del Vecchio[2].

[1] Institute of Biostructures and Bioimages, National Research Council, Naples, Italy.

[2] Department of Advanced Biomedical Sciences, University of Naples "Federico II", Naples, Italy.

[3] Department of Clinical Medicine and Surgery, University of Naples "Federico II", Naples, Italy.

[4]CRCTR Coordinating Rare Tumors Reference Center of Campania Region, AOU "Federico II", Naples, Italy.

Correspondence:

Prof. Silvana Del Vecchio, Via Sergio Pansini 5, 80131 Naples, Italy; phone +390817463307; Fax: +390815457081, e-mail: delvecc@unina.it

First Author:

Prof. Rosa Fonti, Via Tommaso De Amicis 95, 80145, Naples, Italy; phone +390817463307; Fax: +390815457081, e-mail: rosa.fonti@ibb.cnr.it

The authors have nothing to disclose

Word count of the manuscript: 5130

RUNNING TITLE: SSTR2 heterogeneity assessed by CoV

ABSTRACT

High levels of somatostatin receptor type 2 (SSTR2) is a prerequisite for therapy with unlabeled or labeled somatostatin analogues. However, it is still unclear how the heterogeneity of SSTR2 expression could affect tumor response to therapy. The aim of our study was to test the ability of an imaging parameter such as coefficient of variation (CoV) derived from PET/CT with ^{68}Ga-peptides in the evaluation and quantification of the heterogeneity of SSTR2 expression within primary and metastatic lesions of patients with neuroendocrine tumors. **Methods:** Thirty-eight patients with pathologically proven neuroendocrine tumors who underwent ^{68}Ga-DOTATOC-PET/CT were studied. Primary tumors were localized in the gastroenteropancreatic, bronchopulmonary and other anatomical districts in 25, 7 and 6 patients, respectively. Malignant lesions were segmented using an automated contouring program and a threshold of SUV> 2.5 or in the case of liver lesions a threshold of 30% of the SUVmax. The imaging parameters SUVmean, CoV, SUVmax, RETV (receptor expressing tumor volume) and TLRE (total lesion receptor expression) of each lesion were obtained. SUVmean, CoV, SUVmax were also obtained in representative volumes of normal liver, spleen as well as in the whole pituitary gland. **Results:** A total of 107 lesions were analyzed including 35 primary tumors, 32 metastatic lymph nodes and 40 distant metastases. Average CoV values were 0.49±0.20 in primary tumors, 0.57±0.26 in lymph node metastases and 0.44±0.20 in distant metastases. CoV values in malignant lesions were up to 4-fold higher than those of normal tissues ($p \leq 0.0001$). Among malignant lesions the highest CoV value was found in bone metastases (0.68±0.20) and was significantly greater than that of primary lesions ($p=0.01$) and liver metastases (0<0.0001). On the other hand, the lowest CoV value was found in liver lesions (0.32±0.07) probably due to the high background. **Conclusion:** Our findings indicate that the heterogeneity of tracer uptake, reflecting that of SSTR2, varies depending on type and site of malignant lesions as assessed by CoV values obtained from ^{68}Ga-DOTATOC-PET/CT scans. These observations may be related to different biological

characteristics of tumor lesions in the same patient that may affect their response to treatment with both labeled and unlabeled somatostatin analogues**.**

Key words: somatostatin receptor 2; heterogeneity; coefficient of variation; ^{68}Ga-peptide PET/CT; neuroendocrine tumors.

INTRODUCTION

Neuroendocrine neoplasms are a heterogeneous group of rare tumors arising from the diffuse neuroendocrine cell system that includes both well-differentiated neuroendocrine tumors (NETs) and poorly differentiated carcinomas. Grading of NETs is essentially based on the rate of proliferation as assessed by Ki67 staining (*1*). A common property of well-differentiated NETs is the overexpression of somatostatin receptors that constitute a target for therapy with unlabeled and beta-emitter conjugated somatostatin analogues (*2,3*).

Somatostatin receptors belong to the large family of G protein coupled receptors that upon binding with their specific ligands activate guanosine triphosphate - binding proteins that in turn will propagate signaling cascade using different second messenger systems (*4,5*). Of the 5 known somatostatin receptor (SSTR) subtypes 1-5, the SSTR2 receptor is the most widely distributed in normal tissues and human tumors (*6*). High levels of SSTR2 have been found mainly in grading 1 (G1) and grading 2 (G2) NETs where a heterogeneous pattern of expression was also observed (*7,8*). Although previous studies showed that high levels of SSTR2 could predict a good response to therapy with somatostatin analogues and a prolonged survival (*7,8*), it is still unclear how the heterogeneity of SSTR2 expression within a lesion or among different lesions in the same patient may affect tumor response to therapy and clinical outcome.

SSTR2 display a complex temporal and tissue-specific pattern of expression involving several growth and transcriptional factors, hormones, inflammatory cytokines, specific ligands and microenviromental conditions (*4,9*). More recently, a growing body of evidence indicates that SSTR2 expression can be regulated by epigenetic mechanisms (*10,11*) such as DNA methylation and histone acetylation. Furthermore, upregulation of SSTR2 has been reported to occur through activation of NF-kB and MEK signaling pathways in a model of Epstein Barr infection of nasopharyngeal carcinoma cells (*12*).

In order to test the predictive and prognostic value of intratumoral heterogeneity of SSTR2 expression as well as its possible role in the prediction and evaluation of Peptide Receptor Radionuclide Therapy (PRRT) response, some authors adopted a radiomic approach to extract several features from positron emission tomography/computed tomography (PET/CT) scans performed with ^{68}Ga-labeled analogues (*13-17*). In particular a previous study (*13*) reported that four parameters, i.e. Entropy, Correlation, Short zone Emphasis and Homogeneity were able to predict both progression-free survival and overall survival in patients candidate to PRRT. Furthermore, Receptor Expressing Tumor Volume (RETV) could predict overall survival whereas maximum Standardized Uptake Value (SUVmax) and mean Standardized Uptake Value (SUVmean) did not correlate with survival. In another study (*16*) specific texture features derived from ^{68}Gallium-DOTATOC (^{68}Ga-DOTATOC) and ^{18}F-labeled 2-deoxy-D-glucose (^{18}F-FDG) PET/CT, including intensity variability, size zone variability, zone percentage, entropy, homogeneity, dissimilarity, and coefficient of variation were actually able to predict size, angioinvasion, and lymph node involvement in pancreatic NETs.

Among the texture features for the assessment of tumor heterogeneity, coefficient of variation (CoV) is a simple and easy to calculate first order parameter that indicates the percent variability of SUVmean within the tumor volume reflecting the heterogeneity of tracer distribution and hence SSTR variability in ^{68}Ga-peptide examinations.

Although we are aware that radiomics is a powerful tool to characterize tumor heterogeneity and to extract clinical relevant subvisual information from PET images, the aim of the present study was to test the ability of a first order parameter such as coefficient of variation derived from ^{68}Ga-peptide PET/CT scans to quantify the heterogeneity of SSTR2 expression within primary and metastatic lesions of NET patients.

MATERIALS AND METHODS

Patients

We studied 38 patients (25 men, 13 women; mean age 60±14 years; range 29-80 years) with pathologically proven neuroendocrine tumors who underwent ^{68}Ga-DOTATOC-PET/CT scan at our Institution. The study has been approved by the institutional review board, and all subjects signed an informed consent form. Patients were examined at the time of first diagnosis or during the course of disease and 6 of them were re-examined during follow-up, therefore a total of 44 gallium scans were performed and evaluated. Primary tumor was localized in the gastroenteropancreatic district (25 patients: 16 pancreas, 6 midgut, 3 mesentery), in the bronchopulmonary district (7 patients) or in other anatomical districts (6 patients). Tumor grading and Ki67 proliferation index were available in 30 patients. Among them, 11 patients were classified as G1, 16 as G2 and 3 patients as G3 while, Ki67 was <3% in 11 patients, between 3-20% in 16 and >20% in 3 patients (*1*). Ten patients had primary tumor only, 9 patients had lymph node but not distant metastases and 19 patients showed distant metastases with or without lymph node metastases. Patient characteristics are shown in Table 1. Seventeen ^{68}Ga-DOTATOC-PET/CT scans were performed in patients who had previously undergone surgery. When administered previous treatments such as chemotherapy, temozolomide or everolimus were discontinued at least six months before PET/CT scan. Furthermore, 18 scans were performed in patients under treatment with somatostatin analogues using standard regimen (30 mg i.m. once every 4 weeks) as discontinuation of therapy was not clinically recommended to avoid disease progression. In these patients somatostatin analogues where administered on average ± Standard Deviation (SD) 12.9 ±7.6 days before the PET/CT scan, while the other patients receiving somatostatin analogues discontinued it since more than one month before the scan.

^{68}Ga-DOTATOC Labeling

The radiopharmaceutical was prepared using a commercially available kit (SomaKit TOC, Advanced Accelerator Application, a Novartis Company) containing DOTATOC (edotreotide), a somatostatin analogue with a high affinity for SSTR2. Edotreotide labeling was performed following the manufacturer's instructions. Briefly, ^{68}Ga-chloride eluted directly from a ^{68}Ge/^{68}Ga generator (Eckert & Ziegler Radiopharma GmbH) was added to 40 μg of peptide. The solution was immediately buffered and heated to 95°C for 7 minutes using a hot plate. Finally, the product was cooled down at room temperature before use. All steps were performed under sterile conditions and the final product was subjected to thin layer chromatography to verify labeling efficiency. In all labeling procedures the percentage of free and colloidal ^{68}Ga were ≤ 2% and ≤ 3%, respectively.

^{68}Ga-DOTATOC**-PET/CT Study**

Patients underwent PET/CT scan 60 min after intravenous administration of ^{68}Ga-DOTATOC (mean±SD 135±25 MBq) using an Ingenuity TF scanner (Philips Healthcare, Best, The Netherlands). CT scan was acquired using the following parameters: 120 kV, 80 mA, 0.8 s rotation time, pitch of 1.5. PET scan was acquired in 3D mode, from the top of skull to the upper thigh (3 min/each bed position) from 6 to 8 bed positions per patient, depending on height. Iterative reconstruction of images was performed with an ordered subsets-expectation maximization algorithm. Attenuation corrected emission data were obtained using filtered back projection of CT reconstructed images. The resulting transaxial, sagittal and coronal PET, CT and fusion images were preliminarily examined using the Ingenuity TF software.

^{68}Ga-DOTATOC**-PET/CT Image Analysis**

Images were transferred in DICOM format to a workstation equipped with LIFEx program (*18*). All focal areas not attributable to physiological uptake of ^{68}Ga-DOTATOC that showed morpho-structural alterations on the corresponding CT images were considered as positive. In case of multiple liver or bone metastases, the lesion with the highest SUVmax was analyzed, while coalescent lymph nodes were

considered as a single lesion. A volume of interest (VOI) for each positive lesion was obtained by drawing a three-dimensional region around the lesion using an automatic segmentation method (*19*,*20*) that groups all spatially connected voxels within a predefined threshold. In particular, a threshold of SUV> 2.5 was used in all lesions based on the mean SUVmax value of mediastinal blood pool plus 2 SD, except for liver metastases where, due to the high physiological liver uptake, a threshold of 30% of the SUVmax was used to avoid the inclusion of normal parenchyma in the VOI (*21*,*22*). In addition, the accuracy of tumor delineation was confirmed on the corresponding CT images. By computed analysis of each VOI the following parameters were obtained: SUVmean, CoV (Standard Deviation divided by SUVmean), SUVmax, RETV and Total Lesion Receptor Expression (TLRE) obtained by multiplying SUVmean by RETV. In addition to tumor lesions, normal organs with high physiological tracer uptake were also analyzed, thus obtaining SUVmean, CoV and SUVmax in representative volumes of liver and spleen (using VOIs of the same size) as well as in the entire pituitary gland. Representative images of VOIs drawn around malignant lesions and within normal tissues are shown in Figure 1.

Statistical Analysis

Statistical analysis was performed using MedCalc software for Windows, version 10.3.2.0, (MedCalc Software, Mariakerke, Belgium). A probability value <0.05 was considered statistically significant. Student's t-test was used to compare means of unpaired data.

RESULTS

Forty-four ^{68}Ga-DOTATOC-PET/CT scans were performed in 38 NET patients. A total of 107 lesions were analyzed including: 35 primary tumors (27 gastroenteropancreatic, 5 bronchopulmonary and 3 in other anatomical districts), 32 lymph node metastases (20 regional and 12 non-regional) and 40 distant metastases (21 in the liver, 10 in the bones and 9 in other anatomical sites of which 2 in the pancreas, 3 in

the spleen, 2 in the peritoneum, 1 in the thyroid and 1 in the retroperitoneum) as shown in Table 2. The imaging parameters SUVmean, CoV, SUVmax, RETV and TLRE obtained in primary lesions, lymph node metastases and distant metastases are shown in Table 3. In addition to tumor lesions, normal organs with high physiological tracer uptake such as liver, spleen and pituitary gland were also analyzed and the values of SUVmean, CoV and SUVmax are reported in Table 4.

We first examined the effects of treatment with somatostatin analogues on tracer uptake in both tumor lesions and normal tissues by comparing the SUVmax values obtained in patients undergoing (N=18) or not (N=26) therapy at the time of gallium scan. As shown in Table 5, no statistically significant difference was found between the SUVmax values in malignant lesions (primary tumors, lymph node and distant metastases) of treated and untreated patients. On the contrary, tracer uptake was significantly reduced in normal liver ($p<0.0001$), spleen ($p<0.0001$) and pituitary gland ($p<0.02$) of treated patients. These data indicate that the administration of somatostatin analogues using a standard regimen reduces the physiological uptake of ^{68}Ga-DOTATOC in normal organs without affecting the tracer uptake in malignant lesions. Similarly, neither SUVmean nor CoV in primary lesions ($p=0.3515$ and $p=0.2718$, respectively), lymph node metastases ($p=0.4497$ and $p=0.0748$, respectively) and distant metastases ($p=0.1068$ and $p=0.2128$, respectively) were statistically different between patients under treatment or not. Therefore, the analysis of imaging parameters was performed in all patients as a whole group.

SUVmean values (mean±SD) in primary lesions, lymph node and distant metastases were 8.70±7.53, 8.38±4.10 and 13.72±9.90, respectively (Table 3). There was no statistically significant difference between the SUVmean of primary lesions and lymph node metastases ($p=0.8507$), while both were significantly lower than that of distant metastases ($p=0.0170$ and $p=0.0056$, respectively). Moreover, CoV values in primary lesions, lymph node metastases, and distant metastases were 0.49±0.20, 0.57±0.26 and 0.44±0.20, respectively (Table 3). There were no statistically significant differences between the CoV

of primary lesions and lymph node metastases (p=0.1730) or distant metastases (p=0.3260), while lymph node metastases had a significantly higher CoV than that of distant metastases (p =0.0253).

In a further analysis, distant metastases were divided in three subgroups including liver, bone and other metastatic lesions and for each subgroup SUVmean and CoV values were determined (Table 6). Average SUVmean in liver, bone and other metastatic lesions were 17.09±11.61, 9.61±6.40 and 10.45±5.67, respectively. No statistically significant differences were found between the SUVmean values of the three subgroups of distant metastases. CoV values (mean±SD) of liver, bone and other metastatic lesions were 0.32±0.07, 0.68±0.20 and 0.47±0.15, respectively. Bone metastases had a significantly higher CoV than both liver lesions (p <0.0001) and metastases of other sites (p=0.0269). A significant difference was also found between the CoV values of liver and other metastatic lesions (p=0.0006). Therefore, the greatest heterogeneity of tracer uptake reflecting somatostatin receptor expression was found in bone lesions compared to the other distant metastases.

Furthermore, the CoV value of bone metastases was significantly higher than that of primary lesions (p=0.0132) but not significantly different than that of lymph node metastases (p=0.2330). On the contrary, the CoV of liver metastases was significantly lower than that of primary lesions (p=0.0005) and lymph node metastases (p=0.0001). On the other hand, no statistically significant differences were found between the CoV values of metastases in other sites and primitive lesions (p=0.8327) or lymph node metastases (p=0.3138). Finally, as expected, the mean CoV value of primary lesions, lymph node metastases and distant metastases was significantly higher ($p \leq 0.0001$) than that of normal liver, spleen and pituitary gland.

Values of conventional parameters such as SUVmax and volumetric parameters such as RETV and TLRE obtained in tumor lesions are shown in Table 3. SUVmax values (mean±SD) were 24.10±19.51 in primary lesions, 27.77±20.51 in lymph node metastases and 34.99±27.89 in distant metastases. No

statistically significant differences were found between the SUVmax of these three groups of lesions, although the SUVmax of distant metastases tended to be higher than that of primary lesions (p=0.0573). The mean values of RETV and TLRE were 25.07±34.75 and 309.83±813.83 in primary lesions, 13.26±17.42 and 142.56±195.34 in lymph node metastases, and 33.68±36.04 and 601.23±816.25 in distant metastases, respectively. RETV and TLRE of distant metastases were significantly greater than that of lymph node metastases (p=0.0044 and p=0.0028, respectively) while there were no statistically significant differences between the RETV and TLRE values of primary lesions and lymph node (p=0.0879 and p=0.2616, respectively) or distant metastases (p=0.2972 and p=0.1268, respectively).

DISCUSSION

Our study shows that all malignant lesions had up to 4-fold higher CoV value than normal tissues. In particular, the highest CoV value was found in bone metastases followed by lymph node metastases and primary lesions reflecting the variable expression of somatostatin receptor depending on type and site of the lesion. These findings suggest that, due to receptor heterogeneity among lesions, the biological behavior of tumor cells may vary at different sites leading to different pattern of tumor growth and progression as well as to different response to targeted therapy with somatostatin analogues.

On the other hand, liver metastases, despite having the highest tracer uptake, showed the lowest CoV value among the three groups of distant metastases. The reason could be that metastatic cells infiltrate and proliferate within a tissue with a high and homogeneous physiological uptake such as normal liver. In fact, to avoid the inclusion of normal parenchyma in the tumor VOI, we used a percentage segmentation threshold different from that of all other lesions and the accuracy of the tumor contouring procedure was carefully checked on the corresponding CT images. However, it cannot be ruled out that normal liver parenchyma may be interspersed with clusters of metastatic cells within the lesion.

Previous studies evaluated the heterogeneity of somatostatin receptor expression by texture analysis determining the prognostic value of several texture parameters such as entropy and homogeneity in NET patients (*23,24*). In our study, we used a simple first order parameter such as CoV that was able to reveal and quantitate the heterogeneity of receptor expression in malignant lesions depending on their type and site. Furthermore, our observations may provide methodological clues for texture analysis of NETs since metastatic lesions in different districts cannot be analyzed together because they can have a different predictive value on tumor response and final outcome due to significantly different heterogeneity. Moreover, using a texture analysis approach, repeatability and reproducibility of texture features is a major issue. In this respect CoV measurements depend from the same factors affecting conventional parameters such as SUVmax and SUVmean and we used an automated contouring program to standardize as much as possible the procedure.

The site-dependent pattern of SSTR2 heterogeneity in malignant lesions may be caused by the different microenvironmental conditions at the various sites. Accumulating evidences indicate indeed that a dynamic cross-talk exists between NETs cells and tumor stroma since NET cells produce a large spectrum of pro-angiogenic and pro-fibrotic factors inducing a high intratumoral microvascular density and fibrotic complications whereas stromal cells such as fibroblasts, endothelial and inflammatory cells produce several growth factors and cytokines that can modulate proliferation and likely receptor expression in NET cells (*9*).

In our study, we also evaluated the possible effect of therapy with somatostatin analogues on the uptake of ^{68}Ga-peptide in tumor lesions and normal tissues. We showed that there were no significant differences between the SUVmax values of treated and untreated patients in primary lesions, lymph node and distant metastases while, SUVmax values were significantly lower in normal liver, spleen and pituitary gland of treated patients as compared to those untreated. These findings indicate that the

administration of standard doses of somatostatin analogues reduces the uptake of ^{68}Ga-peptide in high capacity/low affinity compartments such as normal liver and spleen, while has no detectable effects on the uptake of low capacity/high affinity compartments such as malignant lesions. It is likely that the standard doses of peptide usually prescribed to NET patients do not reach the large excess of cold peptide probably needed to compete with ^{68}Ga-peptide for receptor binding in tumor cells. On the other hand, it is well known that binding of somatostatin analogues to SSTR2 is followed by receptor internalization and this process may reduce receptor density on the plasma membrane. However, there are evidences that prolonged treatment with somatostatin analogues may cause receptor upregulation (*5*) probably depending on cell context and microenviromental conditions. These findings taken together may be useful in the clinical practice, as discontinuation of therapy with somatostatin analogues in patients undergoing PET/CT with ^{68}Ga peptides could be avoided without affecting the results of the diagnostic scan.

CONCLUSION

Our study shows that a simple parameter obtained by ^{68}Ga-DOTATOC-PET/CT image analysis such as CoV allows the evaluation of tracer uptake heterogeneity in tumor lesions located in different anatomical districts. The heterogeneity of tracer uptake reflects that of somatostatin receptor expression and therefore may be related to different biological characteristics of tumor lesions in the same patient potentially predicting differential tumor response to treatment with both labeled and unlabeled somatostatin analogues.

DISCLOSURES

No personal grants, consulting fees, or honoraria are involved in the present manuscript.

The authors declare no conflicts of interest.

KEY POINTS

Question: Can heterogeneity of SSTR2 expression be easily evaluated by ^{68}Ga-peptide PET/CT in a clinical context?

Pertinent Findings: Heterogeneity of SSTR2 was measured by CoV derived from ^{68}Ga-peptide PET/CT performed in NET patients. The highest CoV value was found in bone metastases followed by lymph node metastases and primary lesions.

Implications for Patient Care: The heterogeneity of ^{68}Ga-DOTATOC uptake, reflecting that of SSTR2, varies depending on type and site of malignant lesions and may affect the response to treatment with both labeled and unlabeled somatostatin analogues.

REFERENCES

1. Pavel M, Öberg K, Falconi M, et al. Gastroenteropancreatic neuroendocrine neoplasms: ESMO clinical practice guidelines for diagnosis, treatment and follow-up. *Ann Oncol.* 2020;31:844-860.
2. Strosberg J, El-Haddad G, Wolin E, et al. Phase 3 trial of ^{177}Lu-Dotatate for midgut neuroendocrine tumors. *N Engl J Med*. 2017;376:125-135.
3. Kong G, Hicks RJ. Peptide Receptor Radiotherapy: Current approaches and future directions. *Curr Treat Options Oncol.* 2019;20:77.
4. Barnett P. Somatostatin and somatostatin receptor physiology. *Endocrine.* 2003;20:255-264.
5. Olias G, Viollet C, Kusserow H, Epelbaum J, Meyerhof W. Regulation and function of somatostatin receptors. *J Neurochem.* 2004;89:1057-1091.
6. Reubi JC, Waser B. Concomitant expression of several peptide receptors in neuroendocrine tumours: molecular basis for in vivo multireceptor tumour targeting. *Eur J Nucl Med Mol Imaging*. 2003;30:781-793.
7. Qian ZR, Li T, Ter-Minassian M, et al. Association between somatostatin receptor expression and clinical outcomes in neuroendocrine tumors. *Pancreas*. 2016;45:1386-1393.
8. Hu Y, Ye Z, Wang F, et al. Role of somatostatin receptor in pancreatic neuroendocrine tumor development, diagnosis, and therapy. *Front Endocrinol*. 2021;12:679000.
9. Cives M, Pelle' E, Quaresmini D, Rizzo FM, Tucci M, Silvestris F. The tumor microenvironment in neuroendocrine tumors: biology and therapeutic implications. *Neuroendocrinology*. 2019;109:83-99.
10. Klomp MJ, Dalm SU, de Jong M, Feelders RA, Hofland, Hofland LJ. Epigenetic regulation of somatostatin and somatostatin receptors in neuroendocrine tumors and other types of cancer. *Rev Endocr Metab Disord*. 2021;22:495-510.

11. Taelman VF, Radojewski P, Marincek N, et al. Upregulation of key molecules for targeted imaging and therapy. *J Nucl Med.* 2016;57:1805-1810.

12. Lechner M, Schartinger VH, Steele CD, et al. Somatostatin receptor 2 expression in nasopharyngeal cancer is induced by Epstein Barr virus infection: impact on prognosis, imaging and therapy. *Nat Commun*. 2021;12**:**117.

13. Werner RA, Lapa C, Ilhan H, et al. Survival prediction in patients undergoing radionuclide therapy based on intratumoral somatostatin-receptor heterogeneity. *Oncotarget.* 2017;8:7039-7049.

14. Önner H, Abdülrezzak U, Tutuş A. Could the skewness and kurtosis texture parameters of lesions obtained from pretreatment Ga-68 DOTA-TATE PET/CT images predict receptor radionuclide therapy response in patients with gastroenteropancreatic neuroendocrine tumors? *Nucl Med Commun.* 2020;41:1034-1039.

15. Weber M, Kessler L, Schaarschmidt B, et al. Treatment-related changes in neuroendocrine tumors as assessed by textural features derived from ^{68}Ga-DOTATOC PET/MRI with simultaneous acquisition of apparent diffusion coefficient. *BMC Cancer.* 2020;20**:**326.

16. Mapelli P, Partelli S, Salgarello M, et al. Dual tracer 68Ga-DOTATOC and ^{18}F-FDG PET/computed tomography radiomics in pancreatic neuroendocrine neoplasms: an endearing tool for preoperative risk assessment. *Nucl Med Commun.* 2020;41:896-905.

17. Liberini V, Rampado O, Gallio E, et al. ^{68}Ga-DOTATOC-PET/CT-based radiomic analysis and PRRT outcome: a preliminary evaluation based on an exploratory radiomic analysis on two patients. *Front Med.* 2021;7:601853.

18. Nioche C, Orlhac F, Boughdad S, et al. LIFEx: A freeware for radiomic feature calculation in multimodality imaging to accelerate advances in the characterization of tumor heterogeneity. *Cancer Res*. 2018;78:4786-4789.

19. Fonti R, Larobina M, Del Vecchio S, et al. Metabolic tumor volume assessed by ^{18}F-FDG PET/CT for the prediction of outcome in patients with multiple myeloma. *J Nucl Med*. 2012;53:1829-1835.

20. Pellegrino S, Fonti R, Mazziotti E, et al. Total metabolic tumor volume by ^{18}F-FDG PET/CT for the prediction of outcome in patients with non-small cell lung cancer. *Ann Nucl Med*. 2019;33:937-944.

21. Fonti R, Conson M, Del Vecchio S. PET/CT in radiation oncology. *Semin Oncol.* 2019;46:202-209.

22. Liberini V, De Santi B, Rampado O, et al. Impact of segmentation and discretization on radiomic features in ^{68}Ga-DOTA-TOC PET/CT images of neuroendocrine tumor. *EJNMMI Physics*. 2021;8:21.

23. Bezzi C, Mapelli P, Presotto L, et al. Radiomics in pancreatic neuroendocrine tumors: methodological issues and clinical significance. *Eur J Nucl Med Mol Imaging.* 2021;48:4002-4015.

24. Saleh M, Bhosale PR, Yano M, et al. New frontiers in imaging including radiomics updates for pancreatic neuroendocrine neoplasms. *Abdom Radiol (NY)*. 2020; Epub ahead of print.

GRAPHICAL ABSTRACT

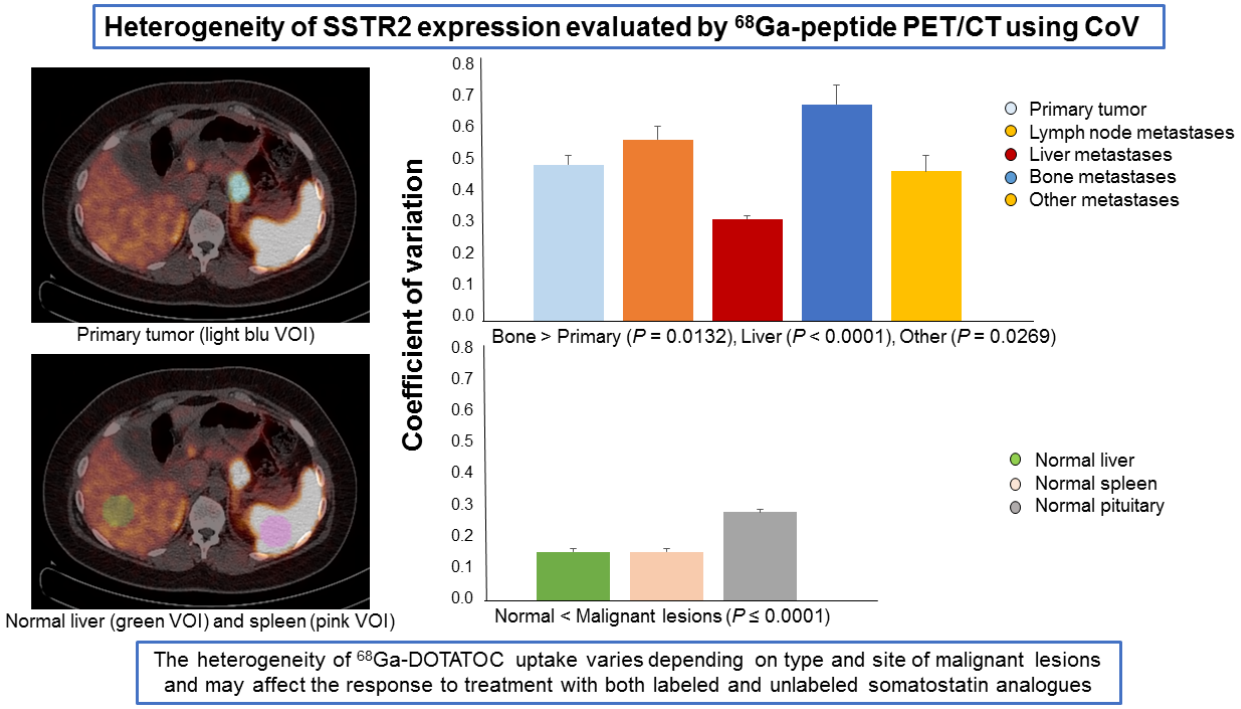

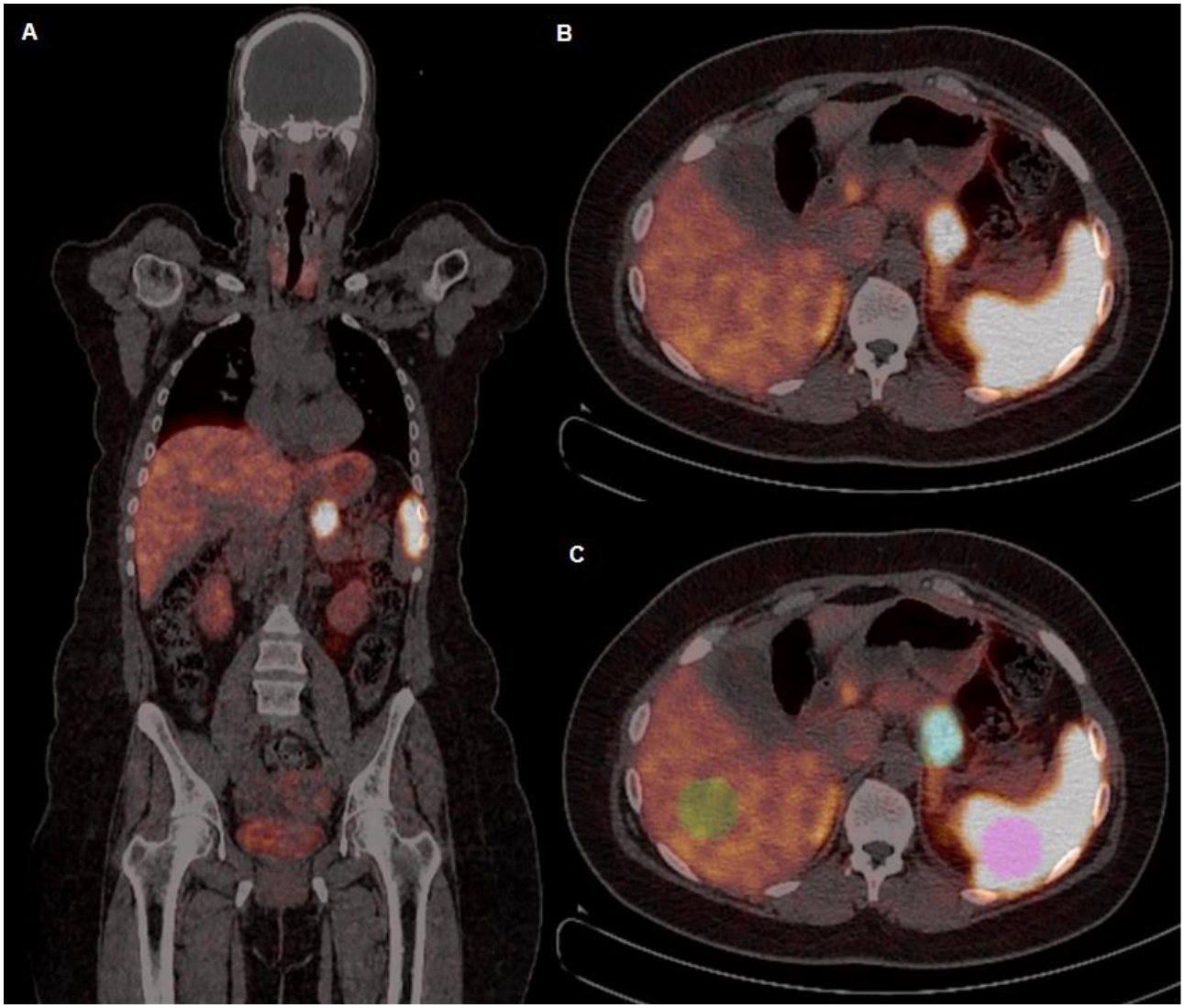

FIGURE 1. ^{68}Ga-DOTATOC-PET/CT in a patient with pancreatic NET. Coronal fusion image showing the primary tumor (A). Transaxial fusion images of the same section without (B) and with (C) overlay of volumes of interest drawn around primary tumor (blu VOI), within normal liver (green VOI) and within normal spleen (pink VOI).

TABLE 1. Patients characteristics.

Characteristics	Value
Patients	38
Age	
Mean±SD*	60±14 y
Range	29-80 y
Gender	
Female	13 (34%)
Male	25 (66%)
Type of NET†	
GEP‡	25 (66%)
BP§	7 (18%)
Other	6 (16%)
Grading	
G1	11 (29%)
G2	16 (42%)
G3	3 (8%)
n.d.‖	8 (21%)
Ki67 (%)	
< 3	11 (29%)
3-20	16 (42%)
> 20	3 (8%)
n.d.	8 (21%)
Lesion sites per patient	
Primary tumor only	10 (26%)
Primary tumor + lymph node metastases	6 (16%)
Primary tumor + distant metastases	6 (16%)
Primary tumor + lymph node metastases + distant metastases	6 (16%)
Lymph node metastases only	3 (8%)
Distant metastases only	3 (8%)
Lymph node metastases + distant metastases	4 (10%)

*Standard Deviation; †Neuroendocrine Tumor; ‡Gastroenteropancreatic; §Bronchopulmonary; ‖not determined.

TABLE 2. Type and number of lesions analysed on ^{68}Ga-DOTATOC-PET/CT images.

Lesions	Number
Primary tumor	**35**
Gastroenteropancreatic tract	27
Bronchopulmonary tract	5
Other sites	3
Lymph node metastases	**32**
Regional basins	20
Non regional basins	12
Distant Metastases	**40**
Liver	21
Bone	10
Other sites	9
Total lesions	**107**

TABLE 3. Imaging parameters obtained by ^{68}Ga-DOTATOC-PET/CT analysis of primary tumors, lymph node and distant metastases.

Parameter	Mean ± SD*	Median	Range	*P#*
SUVmax†				
Primary tumor (T)	24.10 ± 19.51	16.60	4.78 - 88.31	T vs N = 0.4559
Lymph node metastases (N)	27.77 ± 20.51	21.51	3.00 - 82.04	N vs M = 0.2256
Distant metastases (M)	34.99 ± 27.89	28.26	3.98 - 115.55	M vs T = 0.0573
SUVmean‡				
Primary tumor (T)	8.70 ± 7.53	6.86	3.29 - 42.72	T vs N = 0.8507
Lymph node metastases (N)	8.38 ± 4.10	8.05	1.41 - 18.31	N vs M = 0.0056
Distant metastases (M)	13.72 ± 9.90	12.44	1.68 - 43.41	M vs T = 0.0170
CoV§				
Primary tumor (T)	0.49 ± 0.20	0.51	0.17 - 0.95	T vs N = 0.1730
Lymph node metastases (N)	0.57 ± 0.26	0.58	0.10 - 1.07	N vs M = 0.0253
Distant metastases (M)	0.44 ± 0.20	0.39	0.14 - 1.00	M vs T = 0.3260
RETV‖ (mL)				
Primary tumor (T)	25.07 ± 34.75	10.69	2.43 - 178.24	T vs N = 0.0879
Lymph node metastases (N)	13.26 ± 17.42	7.04	0.80 - 82.04	N vs M = 0.0044
Distant metastases (M)	33.68 ± 36.04	18.97	2.11 - 136.25	M vs T = 0.2972
TLRE¶ (g)				
Primary tumor (T)	309.83 ± 813.83	63.29	15.80 - 4766.19	T vs N = 0.2616
Lymph node metastases (N)	142.56 ± 195.34	71.25	2.99 - 766.21	N vs M = 0.0028
Distant metastases (M)	601.23 ± 816.25	258.38	3.56 - 2908.85	M vs T = 0.1268

*Standard Deviation; †maximum Standardized Uptake Value; ‡mean Standardized Uptake Value; §Coefficient of Variation; ‖Receptor Expressing Tumor Volume; ¶Total Lesion Receptor Expression; #Unpaired T-test.

TABLE 4. Imaging parameters obtained by ^{68}Ga-DOTATOC-PET/CT analysis of normal organs with high physiological tracer uptake such as liver, spleen and pituitary gland.

Parameter	Mean ± SD*	Median	Range
SUVmax†			
Liver	9.07 ± 3.45	9.37	3.12 - 19.90
Spleen	24.56 ± 11.61	21.89	5.23 - 46.35
Pituitary gland	6.03 ± 2.58	5.88	0.99 - 12.00
SUVmean‡			
Liver	5.94 ± 2.60	5.82	1.84 - 11.27
Spleen	18.48 ± 9.71	18.89	3.00 - 35.63
Pituitary gland	3.95 ± 0.74	3.89	1.13 - 5.30
CoV§			
Liver	0.16 ± 0.07	0.14	0.06 - 0.44
Spleen	0.16 ± 0.09	0.14	0.06 - 0.56
Pituitary gland	0.29 ± 0.11	0.26	0.09 - 0.63

*Standard Deviation; †maximum Standardized Uptake Value; ‡mean Standardized Uptake Value; §Coefficient of Variation;

Table 5. SUVmax values in malignant lesions and normal tissues in patients treated or not with somatostatin analogues.

	NO SSA* THERAPY SUVmax† (mean±SD‡)	SSA THERAPY SUVmax (mean±SD)	*P*
Primary lesions	25.08 ± 22.49	22.44 ± 13.75	n.s§
Lymph node metastases	22.22 ± 22.25	31.57 ± 18.89	n.s
Distant metastases	22.49 ± 13.97	40.34 ± 30.74	n.s.
Normal liver	10.76 ± 3.11	6.55 ± 2.21	< 0.0001
Normal spleen	32.40 ± 8.92	15.49 ± 6.69	< 0.0001
Normal pituitary	7.03 ± 2.18	4.48 ± 2.43	< 0.02

*Somatostatin Analogues; †maximum Standardized Uptake Volume; ‡Standard Deviation; §not significant.

Table 6. Imaging parameters obtained by ^{68}Ga-DOTATOC-PET/CT analysis of liver, bone and other distant metastases.

Parameter	Mean ± SD*	Median	Range	*P*‖
SUVmax†				
Liver metastases (L)	37.98 ± 31.13	28.49	6.87 - 115.55	L vs B = 0.8234
Bone metastases (B)	35.33 ± 29.61	18.83	3.98 - 94.90	B vs O = 0.5038
Other metastases (O)	27.61 ± 17.27	34.72	5.36 - 51.79	O vs L = 0.3586
SUVmean‡				
Liver metastases (L)	17.09 ± 11.61	13.40	4.47 - 43.41	L vs B = 0.0684
Bone metastases (B)	9.61 ± 6.40	6.19	1.68 - 21.85	B vs O = 0.7651
Other metastases (O)	10.45 ± 5.67	14.23	3.43 - 16.54	O vs L = 0.0600
CoV§				
Liver metastases (L)	0.32 ± 0.07	0.33	0.14 - 0.46	L vs B < 0.0001
Bone metastases (B)	0.68 ± 0.20	0.61	0.42 - 1.00	B vs O = 0.0269
Other metastases (O)	0.47 ± 0.15	0.50	0.20 - 0.65	O vs L = 0.0006

*Standard Deviation; †maximum Standardized Uptake Value; ‡mean Standardized Uptake Value; §Coefficient of Variation; ‖ Unpaired T-test.